Gravitational self-force: orbital mechanics beyond geodesic motion

Leor Barack

Abstract The question of motion in a gravitationally bound two-body system is a longstanding open problem of General Relativity. When the mass ratio η is small, the problem lends itself to a perturbative treatment, wherein corrections to the geodesic motion of the smaller object (due to radiation reaction, internal structure, etc.) are accounted for order by order in η, using the language of an effective *gravitational self-force*. The prospect for observing gravitational waves from compact objects inspiralling into massive black holes in the foreseeable future has in the past 15 years motivated a program to obtain a rigorous formulation of the self-force and compute it for astrophysically interesting systems. I will give a brief survey of this activity and its achievements so far, and will identify the challenges that lie ahead. As concrete examples, I will discuss recent calculations of certain conservative post-geodesic effects of the self-force, including the $O(\eta)$ correction to the precession rate of the periastron. I will highlight the way in which such calculations allow us to make a fruitful contact with other approaches to the two-body problem.

1 Background: the self-force domain of the 2-body problem and astrophysical relevance

In Newtonian gravity, the dynamics of a two-body system is extremely simple: an isolated system of two gravitationally-bound point masses admits two conserved integrals—the energy and angular momentum—and the resulting motion is precisely periodic. The corresponding general-relativistic problem is radically more difficult. In General Relativity (GR), the orbits in a bound binary are *never* periodic: gravitational radiation removes energy and angular momentum from the system, and the radiation back-reaction gradually drives the two objects tighter together un-

Leor Barack

School of Mathematics, University of Southampton, Southampton, SO17 1BJ, United Kingdom, e-mail: leor@soton.ac.uk

til they eventually merge. It is testimony to the intricacy of the problem, that this qualitative picture of radiative damping has been fiercely debated in the literature until well into the 1960s (with some results famously predicting an energy *gain* in binary systems emitting waves!). Work by Hermann Bondi and others in the early 1960s eventually settled the dispute, and the prevailing view was later fully vindicated with the 1975 Nobel-Prize observation by Hulse and Taylor of radiative decay in the binary pulsar PSR 1913+16 [1], consistent with Einstein's quadrupole formula.

The dynamics in the Hulse-Taylor binary is very nearly Newtonian, due to the relatively large separation between the two components. We now know that the universe around us abounds with much more strongly gravitating systems, from pairs of inspiralling white dwarfs in nearby galaxies (likely progenitors of most Type Ia supernovae) to the dramatic coalescence of supermassive black holes at cosmological distances—by far the brightest events in the universe by energy output. In the coming years, direct observations of gravitational waves (GWs) will open a new window on the universe and allow us to peer deeply into these strong-field processes, which are largely invisible in electromagnetic spectrum. This is an exciting prospect, because GWs from coalescing compact binaries and black holes will probe the hitherto unexplored strong-field, highly-dynamical sector of Einstein's theory, where a variety of exotic nonliner effects manifest themselves. With this prospect comes the need to have an accurate theoretical model of the two-body dynamics in the strong-field regime, and a prediction of the emitted gravitational waveforms. These waveforms are needed not only to allow interpretation of the signals and facilitate precision tests of GR theory, but also to enable the very extraction of some of the weaker signals from the noisy detector output.

In general, the description of the nonlinear strong-field dynamics in the binary system entails a full Numerical-Relativistic (NR) treatment, whereby the Einstein field equations are formulated as an initial/boundary problem and solved numerically. Efforts to obtain numerical solutions for (in particular) black hole binaries date back to work in the 1960s and 1970s [2, 3], but it was not until 2005 that first successful simulations were performed [4, 5, 6]. Today NR codes are capable of tracking the complicated nonlinear evolution of a spacetime containing two (spinning) black holes during the final stages of the merger. But NR methods have a limited utility in situations where the two black holes are far apart, or when one of the components is much heavier than the other. Each of these two regimes of the two-body problem (see Fig. 1) is characterized by two greatly separate lengthscales (the distance between the objects vs. their individual radii of curvature in the former case; the radius of curvature of the larger black hole vs. that of the smaller one in the latter case), which is difficult to accommodate in an NR framework due to the high resolution requirements and long evolution time.

Fortunately, the presence of two separate lengthscales also means that the problem becomes amenable to a simpler, perturbative treatment. In the first of the above regimes—at sufficiently large separations—the dynamics is best analyzed using the tools of *post-Newtonian* (PN) theory [7], whose roots go as far back as 1938, to the classical paper by Einstein, Infeld and Hoffman's [8]. In PN theory, corrections to
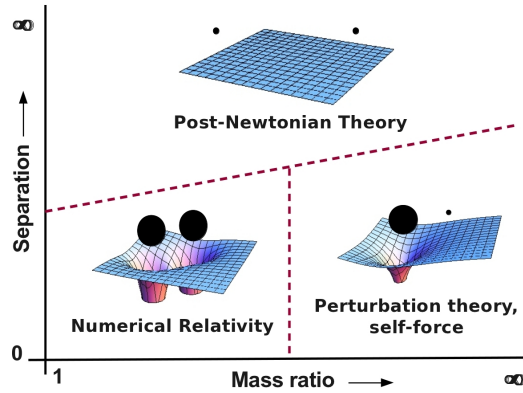
Fig. 1 Schematic representation of the three domains of the binary black-hole problem, with the corresponding natural computational frameworks. Numerical solutions of the full Einstein equations are effectual for very close binaries of comparable masses. Widely separated binaries are treated most efficiently using the tools of post-Newtonian theory (less so when the mass ratio is extreme). Strongly gravitating binaries of large mass ratios are the realm of self-force theory. Much current study focuses on comparing the predictions of the different approaches where they interface (dashed lines).

the Newtonian dynamics are incorporated into the equations of motion (essentially) order by order in the binary separation. PN results are useful (a priori) only when the binary separation is not too small, but no assumption is made about the masses of the two objects, which can be kept arbitrary.

The second, so-called *extreme mass-ratio* regime, is most naturally explored within the framework of black hole perturbation theory. Here the "zeroth-order" configuration is that of a test particle moving along a geodesic of the fixed, stationary background spacetime of the larger object (say, a black hole). This can then serve as a basis for a perturbative scheme, whereby corrections due to the finite mass of the small object (and due also, ultimately, to its internal structure) are included order by order in the small mass-ratio η. At $O(\eta)$, the gravitational field of the small object is a linear perturbation of the background geometry. The back-reaction from this perturbation gives rise to an effective *gravitational self-force* (GSF) that gradually diverts the small object from its geodesic motion. In this picture, it is the GSF that is responsible for the radiative decay of the orbit. It is also responsible for a variety of conservative effects arising from finite-η corrections to the background gravitational potential. The GSF description is useful (a priori) when η is sufficiently small, but the separation between the two objects need not be large. Indeed, GSF theory covers precisely the domain accessible to neither NR nor PN: strongly gravitating binaries of small η.

The basic notion of a "self-force" (aka *back-reaction* force or *braking* force) in a radiating system is an old one, dating many decades back, in the context of electrodynamics, to the classical works by Lorentz [9] and Dirac [10] on the electron's equation of motion. In 1960 DeWitt and Brehme generalized this idea to GR by

deriving an equation of motion for an electric charge moving in curved space [11]. Their method involved a careful application of Gauss's theorem on a thin worldtude surrounding the particle's worldline, with an imposition of local energy-momentum conservation. This work has a fundamental importance also in that it develops the essential mathematical toolkit underpinning contemporary GSF theory: the calculus of bi-tensors in curved spacetime.

The failure of the Huygens principle in 3+1D curved spacetime means that the self-interaction effect in GR is fundamentally *nonlocal*: the self-acceleration formally depends on the entire past history of the particle in question. This represents a significant departure from the flat-space case, and it brings about significant complications, technical as well as conceptual. The application of the self-force idea to the motion of a *mass* particle in GR presents several more complications. Not least among these is the fact that the very notion of a point mass is ill-defined in GR [12]. A rigorous derivation of the GSF equations of motion cannot, therefore, rely on a point-mass assumption, as conveniently done in a linear theory like electrodynamics. For many years, a robust formulation of the GSF remained an open problem in GR theory.

Interest in the problem grew in the mid 1990s, when it was proposed that the planned space-based GW detector LISA (Laser Interferometer Space Antenna [13]) could observe signals from the inspiral of compact objects into massive black holes in galactic nuclei. (The inspiraling objects need be compact—white dwarfs, neutron stars of stellar-mass black holes—because main-sequence stars will be tidally destroyed before they can produce an interesting GW signal.) Later work confirmed that a LISA-like mission should be able to detect hundreds of events, out to cosmological distances ($z \sim 1$) [14]. Dubbed *EMRI*s (Extreme Mass Ratio Inspirals), these sources have a unique facility as precision probes of strong-field gravity. In a typical LISA-band EMRI (a $\sim 10 M_\odot / 10^6 M_\odot$ system), the inspiralling object spends the last few years of inspiral in a very tight orbit around the massive hole, emitting some 10^5–10^6 gravitational wave cycles. The inspiral trajectories show extreme versions of periastron precession, Lense-Thirring precession of the orbital plane, and other strong-field effects. This complex dynamics is encoded in the GWs, which then carry a detailed map of the spacetime geometry around the massive hole. It was calculated, for example, that LISA will be able to measure fractional deviations as small as 1:1000 in the quadrupole moment of the black hole metric [15], allowing precision tests of GR and setting tight bounds on the parameters of alternative theories of gravity.

It is a crucial prerequisite for realizing this science potential that accurate theoretical templates of the inspiral waveforms are at hand. This, in turn, requires a detailed understanding of the radiative evolution. In a typical LISA-band EMRI, the GSF drives the orbital decay over a timescale of months, and it *dephases* the orbit over mere hours. A useful model of the long-term orbital phase evolution therefore ought to account properly for GSF effects, which one must be able to calculate for generic (eccentric, arbitrarily inclined) strong-field orbits around a Kerr black hole of arbitrary spin.

2 The GSF program: foundation

The EMRI problem provided an important impetus to rapid progress in GSF research. In 1997 Mino, Sasaki and Tanaka [16] derived (what has since been "canonized" as) the formal expression for the $O(m^2)$ GSF [that is, the $O(m)$ self-acceleration] acting on a particle of mass m moving in an arbitrary vacuum spacetime of characteristic radius of curvature $\mathscr{R} \gg m$. The expression was derived using two methods (a third, axiomatic method was presented around the same time by Quinn and Wald [17], leading to the same result). The first method was a direct application of DeWitt and Brehme's analysis to the gravitational case, assuming from the onset that the particle can be represented as a point source to the perturbed Einstein equations. The second method removed this assumption: the small object was taken to be a (Schwarzschild) black hole, and its representative "worldline" on the background spacetime was defined and derived using the procedure of *matched asymptotic expansions*.

In its general form, matched asymptotic expansions in a common tool in physics for studying problem involving multiple scales (most relevantly, it has been applied in PN theory [18]). In the particular implementation of [16], the equation of motion is obtained by matching together two series representations of the metric: a "far field" expansion in m/r (where r is a suitable measure of spatial distance from the small black hole), and a "near" field expansion in $r/\mathscr{R}$. The first expansion treats the field of the small black hole at $r \gg m$ as a small perturbation on the external geometry, and the second expansion accounts for the background curvature at $r \ll \mathscr{R}$ via the small tidal deformations it induces on the metric of the small black hole. The assumption $m \ll \mathscr{R}$ means there is a "buffer zone" $m \ll r \ll \mathscr{R}$ where both descriptions apply, and demanding that the descriptions agree in this zone constrains the motion of the small black hole. Matching at leading order shows that the $O(m^0)$ motion is a geodesic on the background geometry. Matching at the next order gives the $O(m)$ acceleration of the small black hole on the background geometry, interpreted as a GSF effect. The accelerated "worldline" is defined from a far-field point of view, via a suitable limiting process. In subsequent work [19, 20, 21, 22], this procedure was generalized and put on a more mathematically firm footing. For example, the small object was allowed to possess spin and consist of any form of matter (not necessarily a black hole). The most elegant and rigorous derivation was presented by Gralla and Wald [20], whose analysis derives both near and far zones as certain limits of a *single* global metric. For a thorough and self-contained review of these theoretical developments, see Ref. [19].

At first post-geodesic order in the GSF approximation, the equation of motion has the form

$$mu^\alpha \nabla_\alpha u^\beta = F^\beta_{\text{self}}, \tag{1}$$

where u^α is the particle's four-velocity on the background spacetime, ∇_α is a covariant derivative on the background spacetime, and $F^\beta_{\text{self}} (\propto m^2)$ is the GSF. The above foundational work gives an expression for F^β_{self} in terms of the "tail" part of the physical metric perturbation associated with the point particle—the part arising from the

piece of the Green's function supported *inside* (rather than *on*) the past light-cone of the source. Roughly speaking, it establishes that it is the back-reaction from the *tail* part of the self-field (which is finite) that is responsible for the self-acceleration.

Two comments are in order. First, as is easily seen, the GSF itself is a gauge-dependent notion, and so is the accelerated trajectory in the background geometry: an $O(m)$ gauge transformation in the perturbed geometry results in a *physically distinct* accelerated trajectory. Thus, a meaningful information about the post-geodesic motion is contained only in the *combination* of the GSF and the metric perturbation (in a particular gauge). The above foundational derivations of the GSF all involve a specific gauge choice—the so called *Lorenz gauge* (in which the divergence of the trace-reversed metric perturbation is set to zero). This is a convenient choice because (i) it preserves the local isotropic nature of the particle singularity, and (ii) the perturbation equations in the Lorenz-gauge are fully hyperbolic and admit a well-posed initial-value formulation. It should not be assumed without a careful examination that the GSF is meaningful or well defined in any other given gauge (this has been a source of much confusion and debate in the GSF literature). A gauge transformation formula for the GSF was derived in Ref. [23], which also proposed some criteria for admissible GSF gauges. The topic is further developed in Ref. [24].

A second comment is that Eq. (1) is only guaranteed to hold momentarily at each point along the trajectory. It is quite a separate task to formulate a scheme that faithfully accounts for the long-term evolution of the orbit. A subtlety is that the Lorenz-gauge condition cannot be imposed consistently when the source's worldline is accelerating. Ref. [20] suggested a scheme where the Lorenz-gauge perturbation equations and the equation of motion (1) are solved as a coupled set in a self-consistent manner, without actively imposing the Lorenz gauge conditions (a similar scheme of "gauge relaxation" has been used in PN theory); the gauge violations which would then occur at $O(m^2)$ will presumably be accounted for within a consistent second-order GSF formulation once this becomes available. In a more recent work, Pound [25] has used techniques from singular and multiple-scale perturbation theories in attempt to put the idea of gauge relaxation on sound mathematical footing, but it seems the issue remains somewhat controversial for now. Stronger consensus is likely to be reached soon, with the advent of the second-order GSF formulations (see Sec. 6). In any case, we note that a computation of the local GSF F_{self}^{β} will constitute a necessary input for any ultimate scheme for the long-term evolution of the orbit.

In a 2003 paper [26] Detweiler and Whiting proposed an appealing reinterpretation of Eq. (1) in terms of geodesic motion in a smooth perturbed spacetime. They showed that the GSF F_{self}^{β} can be interpreted as the back-reaction force from a certain smooth metric perturbation $h_{\alpha\beta}^{R}$, which, unlike the "tail" field mentioned above, is a *vacuum* solution of the linearized Einstein equations. The particle can be thought to be moving along a geodesic of $g_{\alpha\beta} + h_{\alpha\beta}^{R}$, where $g_{\alpha\beta}$ is the background metric. The equation of motion is reformulated as

$$m\tilde{u}^{\alpha}\tilde{\nabla}_{\alpha}\tilde{u}^{\beta} = 0, \tag{2}$$

where $\tilde{u}^{\alpha}$ and $\tilde{\nabla}$ are the four-velocity and covariant derivative in $g_{\alpha\beta} + h^R_{\alpha\beta}$. A pedagogical review of this construction is given in Ref. [19]. It should be emphasized that the perturbation $h^R_{\alpha\beta}$ is *not* the particle's physical metric perturbation (for example, it is not causal), but rather a mathematical construct that serves as an *effective* potential for the motion. The two alternative formulations of the post-geodesic motion, Eqs. (1) and (2), are equivalent and both are useful; workers in the field often flip between the two points of view as necessary to highlight different aspects of the problem.

3 The GSF program: computation

3.1 mode-sum regularization

The above formulation is directly applicable to the EMRI problem, where the "large" scale $\mathscr{R}$ is provided by the mass M of the large black hole. A practical method for calculating the GSF for EMRI orbits, known as *mode-sum regularization* was introduced in 2000 [27], and subsequently became the main working framework for GSF calculations in black hole spacetimes. The method is an implementation of the robust formulation discussed above (no extra regularization is introduced), and we shall give a schematic description of it here. A detailed review can be found in Ref. [28].

As mentioned above, the GSF can be interpreted at the effective force due to the Detweiler-Whiting R-field: $F^{\alpha}_{\text{self}} = m\nabla^{\alpha\beta\gamma}h^R_{\beta\gamma}$, where $\nabla^{\alpha\beta\gamma}$ is a suitable derivative operator defined along the particle's worldline in the background metric. (The original mode-sum scheme was formulated in terms of the tail field but we shall use here the equivalent R-field formulation for simplicity.) The R-field itself can be obtained from the subtraction $h^R_{\beta\gamma} = h^{\text{full}}_{\beta\gamma} - h^S_{\beta\gamma}$, where the "full" field is the physical (retarded) solution of the linearized Einstein equation sourced by the particle's energy-momentum, and the "S"-field (for *singular* field) is a particular solution prescribed by Detweiler and Whiting [26]. The fields $h^{\text{full}}_{\beta\gamma}$ and $h^S_{\beta\gamma}$ have the same singular structure near the moving particle, so that their difference, $h^R_{\beta\gamma}$, is a smooth (C^{∞}) function.

In the mode-sum scheme one essentially performs the above subtraction mode-by-mode in a multipole expansion, and the GSF is then reconstructed from a sum over multipole contributions:

$$F^{\alpha}_{\text{self}} = m\nabla^{\alpha\beta\gamma}\sum_{l=0}^{\infty}\left[(h^{\text{full}}_{\beta\gamma})^l - (h^S_{\beta\gamma})^l\right]. \tag{3}$$

Here a superscript 'l' denotes the l-multipole of the corresponding field (defined, as usual in black hole perturbation theory, via integrals over 2-spheres surrounding the *large* black hole), summed over azimuthal ('m') modes. The advantage of the

multipole decomposition is twofold: First, numerical methods in black-hole perturbation theory are usually based on multipole expansions, so that numerical calculations normally output individual modal contributions anyway. Second, and more crucially, each of the individual modal contributions $(h_{\beta\gamma}^{\text{full}})^l$ [or $(h_{\beta\gamma}^S)^l$] is finite and (piecewise) differentiable at the particle's location, which makes the subtraction more manageable in practice.

Now, as first suggested in Ref. [27], Eq. (3) can be put into a more useful form using some analytic input. One can analytically study the large-l behavior of the S-field modes $(h_{\beta\gamma}^S)^l$ and their derivatives at the particle, and it turns out that (generically) the derivatives admit a large-l expansion in $1/l$, whose leading term is of $O(l)$. (The last statement depends somewhat on the gauge, but here we shall ignore this subtlety for simplicity.) If the first few terms in this expansion are known, one can rewrite Eq. (3) in the form

$$F_{\text{self}}^\alpha = m \sum_{l=0}^\infty \left[\nabla^{\alpha\beta\gamma}(h_{\beta\gamma}^{\text{full}})^l - A^\alpha l - B^\alpha - C^\alpha / l \right], \qquad (4)$$

where A^α, B^α and C^α ("regularization parameters") depend on the particle's location and velocity (and on the background spacetime) but not on l; importantly, it was shown [29, 28] that the residue $\sum_{l=0}^\infty \left[\nabla^{\alpha\beta\gamma}(h_{\beta\gamma}^S)^l - A^\alpha l - B^\alpha - C^\alpha / l \right]$ vanishes along any geodesic orbit in Kerr spacetime. The regularization parameters were calculated analytically for generic orbits in Schwarzschild [30] and later for generic orbits in Kerr [29, 28]. With the regularization parameters given analytically, the task of computing the GSF along a given (pre-specified) orbit reduces to that of obtaining the full modes $(h_{\beta\gamma}^{\text{full}})^l$ to serve as input in the mode-sum formula (4). This is usually done numerically, by solving the suitable set of mode-decomposed perturbation equations with retarded boundary conditions, sourced by the particle orbit in question.

Numerical implementations of the mode-sum formula (4) are reviewed in Ref. [28]. Typically, the particle is taken to move on a fixed geodesic orbit, and the perturbation equations are solved for the corresponding source (the back-reaction effect of the GSF on the orbit has only recently been accounted for in a numerical simulation—see Sec. 4 below). The most advanced implementations of mode-sum regularization are capable of computing the GSF along any (bound) geodesic in Schwarzshild spacetime—these codes where presented in Refs. [31, 32] (time-domain version) and [33, 34] (frequency-domain version). There are also calculations in Kerr spacetime [35, 36], but for now they are restricted to the toy model of a scalar-field self-force. (Shah *et al.* recently used mode-sum regularization to compute a certain GSF-related effect on circular equatorial orbit in Kerr spacetime [37], but they have not computed the GSF itself.) Further advance in mode-sum calculations is represented by the recent analytic derivation of higher-order regularization parameters [terms of $O(l^{-2})$ and higher in the large-l decomposition of the singular field at the particle] by Heffernan *et al.* [38, 39]. This now helps accelerate

the convergence of the mode-sum in numerical implementations, leading to much improved precision in GSF calculations.

3.2 Puncture method

This alternative computation method has been in development since 2007 [40, 41, 42]. The idea here is to "regularize" the field equations themselves, rather than (as in the mode-mode method) their solutions. This method works best with time-domain numerical implementations in 2+1 or 3+1 dimensional, and can benefit from recent advances in numerical method for time-domain evolution of hyperbolic equations in GR. Other advantages: the method offers a direct route to the Kerr problem (still a challenge for mode-sum regularization), and it offers a convenient framework for studies of the orbital evolution under the GSF effect. Following is a schematic description of the method as applied to a scalar-field analogue model; a fuller review can be found in Ref. [28].

Let us write the scalar-field equation in the schematic form $\Box\phi^{\text{full}} = S$, where $\Box$ is a suitable wave operator (depending on the scalar-field theory), S is a source term corresponding to a point particle of scalar charge q, and ϕ^{full} is the sought-for retarded solution. Let ϕ^R and ϕ^S be the scalar-field analogues of Detweiler–Whiting's R and S fields, respectively, so that $F^\alpha_{\text{self}} = q\tilde{\nabla}^\alpha\phi^R$ is the scalar-field self-force, with $\tilde{\nabla}^\alpha$ a suitable gradient operator. The implementation of the puncture scheme begins with finding an analytic approximation to ϕ^S, denoted ϕ^P (the "puncture"), with the property that $\phi^P - \phi^S$ and $\tilde{\nabla}^\alpha(\phi^P - \phi^S)$ both vanish along the particle's worldline (the field ϕ^S can be extended globally as convenient). Then the self-force can be computed via $F^\alpha_{\text{self}} = q\tilde{\nabla}^\alpha\phi^{\text{Res}}$ (evaluated at the particle), where the "residual" field is $\phi^{\text{Res}} := \phi^{\text{full}} - \phi^P$. The latter satisfies the "punctured" equation

$$\Box\phi^{\text{Res}} = S - \Box\phi^P := S_{\text{eff}}, \qquad (5)$$

where the "effective source" S_{eff} no longer contains a delta function. The residual non-smoothness of S_{eff} arises from the fact that ϕ^P is only a finite approximation to ϕ^S (a full expression for ϕ^S is not known in explicit form); one can improve the smoothness of S_{eff} by designing a "higher-order" input puncture ϕ^P, for which higher-order derivatives of $(\phi^P - \phi^S)$ also vanish at the particle. High order punctures for the GSF, and corresponding effective sources, were derived in Refs. [43, 44].

The task of computing the self-force now reduces to solving the field equation $\Box\phi^{\text{Res}} = S_{\text{eff}}$ with suitable boundary conditions. One usually truncates (or otherwise attenuates) the support of ϕ^P far from the particle, so that the necessary boundary conditions are the usual "retarded" ones. Several group are now engaged in code development for self-force calculations in the puncture approach. Most work so far has been confined to the toy model of a scalar field (as a platform for code development and testing) [45, 46, 43, 44], but a first implementation of the GSF has

very recently been presents [47] for circular orbits around a Schwarzschild black hole. Existing puncture codes use a 2+1 (or 3+1)-dimensional grid, which avoids the issue of separability of the field equations in Kerr spacetime. This makes the extension of Schwarzschild codes to Kerr rather straightforward. Indeed, following on from [47], a first implementation of the GSF in Kerr will be presented shortly in a forthcoming paper [48].

As mentioned, time-domain codes based on the puncture method provide a natural platform for studying the orbital evolution under the self-force: rather than pre-specifying the orbit, one can compute the self-acceleration at any time slice, then modify the source accordingly "in real time" so as to compute the evolving orbit in a self-consistent manner (say, using the idea of Lorenz-gauge relaxation). Unfortunately, current codes are not sufficiently efficient computationally to track the evolution in an EMRI-relevant system over many orbits. (A first self-consistent evolution simulation was presented recently for the scalar-field self-force [49], but computational cost restricts the ability of the code to compute more than a handful of orbital cycles.) In the past few years, this computational challenge has attracted some interest from experts in Numerical Relativity, leading to several programs to develop custom-built advanced numerical techniques for integrating the perturbation equations with pointlike sources. These include methods based of finite elements [50], adaptive mesh refinement [51], and hyperboloidal slicing [52]. It is hoped that this activity will lead to a dramatic improvement in the computational performance of time-domain GSF codes.

4 Orbital evolution under the GSF effect

An important milestone in the GSF program was reached last year, with a first computation of the long-term orbital evolution under the full (first order) GSF [34]. This computation was based on a frequency-domain implementation of the mode-sum method in Schwarzschild spacetime, developed in [35, 36, 33]. Rather than evolving the orbit in a fully self-consistent manner as described above (which is not easily achievable in a frequency-domain framework), an approximation was used, in which the value of the GSF at each point along the evolving orbit is taken to be that computed along a fixed geodesic tangent to the orbit at that point. This approximation is a good one in situations where the timescale on which the orbit evolves is much longer than the effective "memory" time associated with the tail field that produces the GSF. In an EMRI-relevant strong-field system with $\eta \ll 1$, the former is expected to be larger than the latter by an amount of order $1/\eta \gg 1$ over much of the inspiral; the approximation will cease to be useful only very near the last stable orbit, where the adiabatic inspiral transits to a direct plunge and the orbit evolves quickly. Let us briefly review the method of [34], then present some results for illustration.

The calculation in [34] is a general-relativistic adaptation of the standard method of "variation of parameters", or "osculating orbits", used in celestial mechanics.

In this *osculating geodesics* approach, the inspiral motion is reconstructed from a smooth sequence of tangent geodesics. In practice, this amounts to solving evolution equations for all the orbital elements that characterize the geodesic motion (principal as well as positional), with the driving force provided by the GSF. The necessary GSF information is prepared in advance, in the form of a global interpolation formula based on a dense data grid over the relevant phase space.

Let us give some more detail. Bound geodesics of the Schwarzschild geometry can be parametrized by their semilatus rectum pM and eccentricity e, defined via $r_\pm = pM/(1 \mp e)$, where $r = r_+$ and $r = r_-$ are the apastron and periastron radii, respectively [hereafter (t, r, θ, φ) are standard Schwarzschild coordinates on the background spacetime]. The geodesic motion of a test particle is then described by [53]

$$r = r_g(t; p, e, \chi_0) = \frac{pM}{1 + e\cos[\chi(t) - \chi_0]}, \tag{6}$$

$$\varphi = \varphi_g(t; p, e, \chi_0) = \int_{\chi(0)}^{\chi(t)} \frac{p^{1/2}\, d\chi'}{\sqrt{p - 6 - 2e\cos(\chi' - \chi_0)}}, \tag{7}$$

where $\chi(t)$ is a monotonically increasing parameter along the orbit (a relativistic generalization of mean anomaly), related to t via $d\chi/dt = (p - 2 - 2e\cos v)(1 + e\cos v)^2(p - 6 - 2e\cos v)^{1/2}[(p - 2)^2 - 4e^2]^{-1/2}/(Mp^2)$, with $v := \chi - \chi_0$. Without loss of generality we have assumed that the motion takes place in the equatorial plane ($\theta = \pi/2$), and took $t(\chi_0) = \varphi(\chi_0) = 0$ (i.e., at $t = 0$ the particle is at periastron at $\varphi = 0$). p and e are *principal* elements, which determine the "shape" of the orbit. χ_0 is a *positional* element, which describes the orientation of the major axis. Both principal and positional elements evolve secularly under the effect of the GSF; the secular evolution of p and e is *dissipative*, while that of χ_0 is *conservative*—it describes the precession effect of the GSF. Both principal and positional elements also exhibit quasi-periodic oscillations.

In the osculating geodesics approach, the inspiral motion is described by $r = r_g(t; p(t), e(t), \chi_0(t))$ and $\varphi = \varphi_g(t; p(t), e(t), \chi_0(t))$, where $p(t)$, $e(t)$, $\chi_0(t)$ are called *osculating elements*. The rate of change of these elements is determined from the local self-acceleration (i.e., F^α_{self} per unit m) of the tangent geodesic. Evolution formulas for the osculating elements, given the GSF, where obtained in Refs. [54] (Schwarzschild case) and [55] (Kerr case). These formulas require as input the function $F^\alpha_{\text{self}}(\chi - \chi_0; p, e)$. In the implementation of Ref. [34] this function was obtained from numerical GSF data computed along a sample of 1100 geodesics covering the p, e parameter space. A suitable interpolation model was derived, based a Fourier representation of the χ-dependence and a power-law series ansatz for the p, e dependence. With this GSF input at hand, the evolution equations for $\{p(t), e(t), \chi_0(t)\}$ were then solved numerically starting from some initial values. An example is shown in Fig. 2.
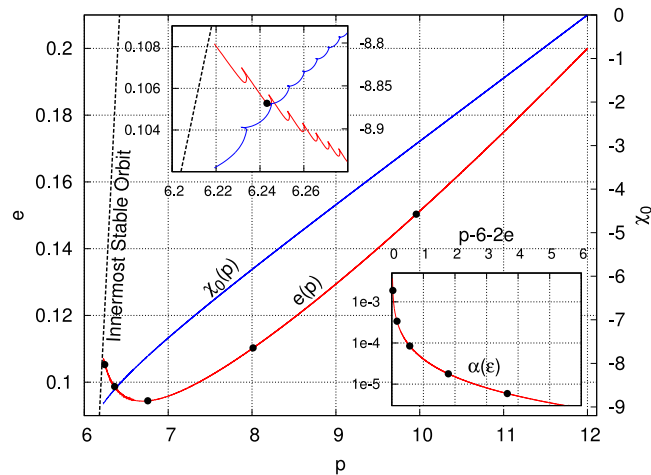
Fig. 2 Evolution of the osculating elements in a sample case with $m = 10M_\odot$ and $M = 10^6 M_\odot$. We show the eccentricity e (red, left axis) and periastron phase χ_0 (blue, right axis) as functions of semi-latus rectum p, as the binary inspirals from $(p,e) = (12, 0.2)$ down to the innermost stable orbit (dashed curve). Marks along the curves count down (from right to left) 500 days, 100 days, 10 days, 1 day and 1 hour to the onset of plunge. Note the orbit initially circularizes, but near the plunge the eccentricity begins to increase. Note also the phase χ_0 decreases monotonically, implying that the conservative GSF acts to *reduce* the rate of relativistic precession. The upper inset is an enlargement of the near-plunge region; the manifest oscillatory behavior is due to the variation of the GSF with the radial phase. The lower inset shows the magnitude of the adiabaticity parameter $\alpha := \langle |\dot{p}/p| \rangle T$ (the average is over a radial period T) vs. the distance $\varepsilon = p - 6 - 2e$ to the innermost stable orbit, confirming that the evolution is strongly adiabatic until very near the end. [Graphics from Ref. [34].]

5 Gauge invariant conservative effects and comparison with other methods

In the last few years GSF results have been used in a variety of applications going beyond the original EMRI program. GSF data can be used to compute gauge-invariant "observables" that describe post-geodesic corrections to the gravitational potential in the two-body system. These can then be utilized as reference points for comparison with the predications of PN theory and with results from full NR simulations. Our current knowledge allows us to go only one order beyond the geodesic approximation [i.e., to $O(\eta)$], but at this order the computed corrections are *exact*, and they give us a direct and hitherto unavailable handle on the very-strong-field conservative dynamics.

What do we mean by "consrevative" dynamics? The precession effect already mentioned is an example. More generally, the GSF can be split in a unique way into dissipative and conservative bits. The dissipative bit is obtained, for example, by replacing $h_{\beta\gamma}^{\text{full}}$ (the retarded metric perturbation) in Eq. (4) with the "half retarded minus half advanced" metric perturbation, and the conservative piece is similarly

obtained from the "half retarded *plus* half advanced" perturbation. (This decomposition bears on time-symmetry and not on secularity: in general, both dissipative and conservative pieces of the GSF would have secular effects on the orbit.) In the simple case of (quasi)circular motion in the equatorial plane of a Kerr black hole, the dissipative piece is given by the coordinate components F_t^{self} and F_φ^{self} (related to dissipation rate of energy and angular momentum, respectively), and the conservative piece is given by F_{self}^r. In more general cases it is still straightforward to construct the two pieces of the GSF separately in practice, either by obtaining both retarded and advanced solutions of the perturbation equations, or (more economically, as described in [28]) by exploiting the time-symmetry of bound geodesics in Kerr spacetime. Indeed, what makes the communication between GSF and PN so natural is the fact that in both approaches (and unlike in NR) the conservative and dissipative aspects of the dynamics can each be studied easily in isolation (this is true at least at first post-geodesic order in the GSF approximation, and through several orders in the PN expansion). In any case, to return to our question, what we mean by *conservative dynamics* is described by solutions to the equation of motion (1), with the GSF on the right-hand side replaced by its conservative piece (or, equivalently, with the dissipative piece "turned off").

A first gauge-invariant "observable" was proposed by Detweiler in 2005 [56]. Considering the effect of the conservative GSF on *circular* orbits in Schwarzschild spacetime, it is easy to see that both components u^t and u^φ of the particle's 4-velocity u^α (on the background spacetime) are invariant through $O(m)$ under $O(m)$ gauge transformations that respect the helical symmetry of the perturbed spacetime. The combination $\Omega := u^\varphi / u^t$, which is the "observable" t-frequency of the perturbed orbit, is obviously also invariant. Detweiler proposed to utilize the $O(m)$ piece of the function $u^t(\Omega)$—let us denote it $u_1^t(\Omega)$—as a concrete gauge-invariant measure of the post-geodesic effect. [A simple calculation shows that $u_1^t(\Omega)$ does not actually involve the GSF itself; rather, it is constructed from the scalar contraction $h_{\alpha\beta}^R u^\alpha u^\beta$, where $h_{\alpha\beta}^R$, recall, is the Detweiler-Whiting R field.] Detweiler also suggested an interpretation of $u_1^t(\Omega)$ as a measure of the GSF correction to the gravitational redshift along a line of sight perpendicular to the orbital plane (but note this interpretation is subtle: the actual redshift from the point particle obviously diverges; rather, it is the redshift defined in the nonphysical effective metric $g_{\alpha\beta} + h_{\alpha\beta}^R$ that this interpretation alludes to). Detweiler used $u_1^t(\Omega)$ as a first contact point with PN theory, showing that the predictions from perturbation theory agree with PN formulas in the weak field [57]. This impressive comparison was pushed to higher-order in the PN expansion in subsequent work [58], also showing how by fitting to GSF data one can derive numerical values for [the $O(m)$ pieces of] higher-order, yet unknown PN coefficients. The quantity $u_1^t(\Omega)$ also served a reference point in a first comparison of GSF calculations carried out in different gauges [59]. Finally, in [60] the notion of redshift variable was generalized to eccentric orbits (using certain orbital averages); preliminary comparison with PN calculations in the eccentric case show a very good agreement [61].

In 2009 Barack and Sago computed the conservative GSF-induced shift in the frequency of the ISCO of a Schwarzschild black hole, using GSF analysis of slightly

perturbed circular orbits [62]. They found, in fractional terms,

$$\left(\frac{\Delta\Omega}{\Omega}\right)_{\text{isco}} = (0.25101546 \pm 0.00000005) \times \eta, \qquad (8)$$

where the uncertainty is due to the finite numerical accuracy of the GSF computation. (We cite here the higher precision value obtained more recently in [63], and we account for a certain gauge correction introduced by Damour in [64], which "regularizes" the Lorenz-gauge time coordinate, known to be otherwise non-asymptotically-flat [65].) This was arguably a first concrete physical result, with a clear physical interpretation, to have emerged from the GSF program. Its importance was in that is provided a long-sought benchmark in the strong field. The ISCO shift result was immediately used as an accurate reference point in an exhaustive study of the performance of various PN methods [66]. It was also used to inform an "empirical" formula (based also on results from NR and PN) for the remnant masses and spins in binary black hole mergers [67], and to constrain some of the analytical parameters of the Effective One Body (EOB) potential [64].

The latter work, especially, highlighted the promise of a synergy between the GSF and other approaches. EOB was introduced by Buonnano and Damour in 1999 [68] as an analytical framework for modelling the two-body dynamics across all mass ratios (see T. Damour's contribution in this volume). At the heart of EOB is an effective one-body Hamiltonian, whose form is chosen to reproduce the known results at the test-particle limit, as well as all known PN results. The EOB Hamiltonian includes a number of "calibration" functions that can be adjusted based available NR data—and now also based of GSF information as it becomes available. In [64] Damour made the point that GSF results are particularly useful for calibrating EOB theory (even more so than NR data) given their accuracy, cleanness, and the fact that conservative effects can be computed separately. In this way, GSF calculations, whose validity is a priori restricted to the extreme mass ratio regime, can indirectly contribute to the development of a universal model of the two-body dynamics across all mass ratios.

In more recent work, Barack and Sago computed the GSF correction to the periastron precession of eccentric orbits around a Schwarzschild black hole [60]. In the limit of zero eccentricity the result is gauge invariant, and can be used it to test the GSF prediction against that of PN theory in the weak field regime. This indeed was done in Ref. [69], where the precession results where also used to improve the calibration of EOB. In a recent culmination of this effort, a 4-way collaboration between groups working on NR, PN, EOB and GSF presented a complete comparison between the predictions of all these methods, using the relativistic precession as a reference point [70]. The results of this study suggest, remarkably, that GSF theory may be applicable well beyond its natural extreme-mass-ratio domain. See Figs. 3 and 4 for an illustration.

In parallel, there has been progress in utilizing Detweiler's redshift variable u_1^α for EOB studies. This followed from a new formulation by Le Tiec and collaborators [71] of a general "first law of binary black hole mechanics", relating infinitesimal
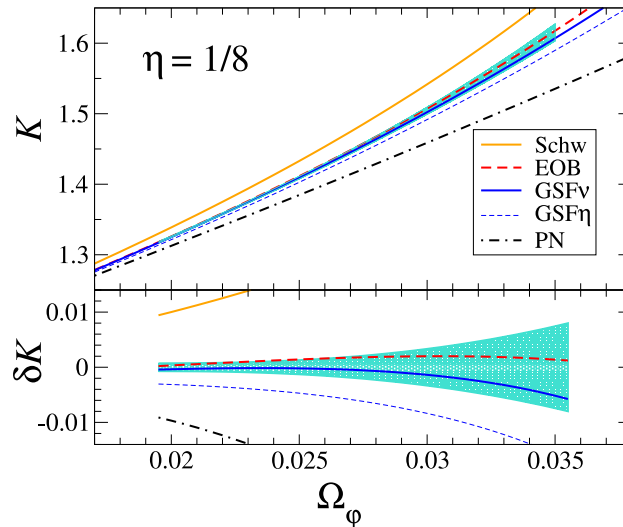
Fig. 3 The relativistic periastron advance per orbit, K, for a close binary of mass ratio $\eta = m{:}M = 1{:}8$. As independent variable we use the invariant frequency Ω_φ, given here in units of inverse-total-mass. (Note the periapsis advances by as much as *half a cycle per radial period* in this extreme regime of GR, corresponding to separations of just a few Schwarzschild radii.) The results, extracted from Ref. [70], show a comparison between the predictions of all methods available today. The shaded region comes from full NR simulations (with error margins), and the lower panel shows the relative difference between the predictions of each approximation method and the NR data. The curve labelled 'Schw' is the test-particle (geodetic) result, given for reference. 'GSFη' refers to the standard GSF prediction, whereas in 'GSFν' the mass ratio η has been replaced with the *symmetric* mass ratio $\nu \equiv mM/(m+M)^2$ [this replacement is "allowed" since $\nu = \eta$ through $O(\eta)$]. 'PN' is the best available (3PN) PN result, and 'EOB' is a certain EOB model (see [70] for details). The GSF approximation, with the replacement $\eta \to \nu$, seems to perform remarkably well even though the mass ratio is not very extreme.

variations of the total (invariant) energy and angular momentum of the binary system to variations of the individual rest masses—a relation which turned out to involve the redshift variable. Further work [72] then related the redshift variable to the EOB potentials, in a way that established a new useful link between GSF data and the EOB functions, leading to a complete determination of two of the main EOB functions at $O(m)$. Most recently [63], this analysis was extended to the very strong-field regime below the ISCO and down to the "light-ring" at $r = 3M$, revealing interesting new features of the EOB potentials.

6 Outlook

The primary ambition of the EMRI program (in the "experimental" context of low-frequency gravitational-wave astronomy) is to obtain a faithful model of the long-
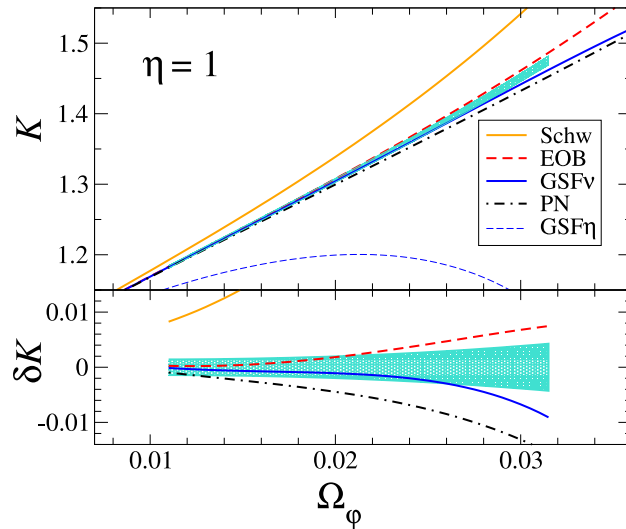
Fig. 4 Same as in Fig. 3, now for $\eta = 1$ (equal masses). Even though this system is a priori well outside the reach of perturbation theory, the GSFν prediction does extremely well, outperforming all other approximation methods. It remains to be seen whether this remarkable agreement is merely fortuitous or representative of a more general behavior.

term orbital evolution in—and emitted gravitational waves from—compact-object binaries of small mass ratios ($\eta \sim 10^{-4}$–10^{-9}), allowing both objects to spin. We are still quite far from achieving this goal. We have accomplished the important prerequisite of being able to compute the leading-order self-acceleration of orbits which are not evolving, in the Schwarzschild background case. But we are yet to learn how to extend this to orbits in Kerr, how to consistently evolve the orbit under the GSF effect, and how to incorporate the second-order GSF and the small object's spin in our calculations (both will be necessary in order to achieve the phase accuracy needed for LISA applications). At the same time, we have learned to appreciate how GSF calculations provide us with new, "high-fidelity" quantitative information about the dynamics in two-body systems, and we are beginning to learn how his can be used to test the faithfulness of PN calculations and inform the development of a universal EOB model. In that, GSF calculations are proving useful far beyond their original motivation. As the field matures, a wider range of applications become apparent. There has been recent work to explore the role of GSF in high-energy black hole scattering (of hypothetical relevance in experimental particle physics) [73, 74], and other applications are foreseeable.

Below we give a brief summary of (what we consider to be) the main challenges that lie ahead in the GSF field.

Foundational issues:— The first-order GSF is well understood at the foundational level, but the situation is less clear at second order. There currently exist at least two independent formulations of the second-order equation of motion, one by Pound [75, 76] and another by Gralla [77]. Both use (variants of) matched asymp-

totic expansions but each chooses to represent the motion in a rather different way, making a direct comparison nontrivial. It is important to understand the relation between the two formulations, and whether they are compatible. It is also important to translate (either or both) of the second-order formulations into a practical computational scheme for the GSF in Kerr geometry—perhaps akin to mode-sum regularization or to the puncture scheme. There is some initial work in this direction, but this problem is likely to remain an important research front for the coming years.

Tightly coupled to the question of a valid second-order formulation is the issue of long-term orbital evolution. Two-timescale expansion methods have been invoked [78, 79] to suggest an evolution scheme and control its error, but it is not yet clear how they would preform in practice (for example, how "runaway" self-acceleration terms would behave in a self-consistent evolution).

Generic inspirals in Kerr experience resonant episodes, where the ratio of the radial and longitudinal orbital frequencies crosses a low-order rational value, and the otherwise ergodic orbit becomes (quasi-)periodic. During resonant epochs radiation reaction acts on quite a different timescale (because the usual "averaging" effect of ergodicity is lost), leading effectively to a sudden jump in the values of the principal orbital elements, and a "resetting" of the orbital phases. If the goal is to obtain accurate phase-coherent waveforms for EMRI systems, it is important to derive an accurate model of the resonant crossing. Some recent work began to address this problem [80, 81, 82].

Computational issues:— A high priority task for the community is to extend existing methods and working codes for GSF calculations in Schwarzschild to a Kerr background. There are two main avenues of approach to the Kerr problem. In the *time-domain* approach one computes the metric perturbation due to the particle by evolving the linearized Einstein equations in the Lorenz gauge on a time-spatial grid using a finite-difference scheme. The 1+1D (time-radial) treatment that works so well in the Schwarzschild case is no longer useful in Kerr, because the Lorenz-gauge perturbation equations in Kerr are not separable (in any known way) into individual multipole modes in the time-domain. Instead, one has to work in 2+1D or 3+1D. This can be done using the puncture method described above, but so far implementations have been restricted to Schwarzschild (refraining from a 1+1D decomposition for the sake of preparing the ground for a Kerr implementation), or to a scalar field. One of the major technical obstacles in moving on to Kerr is the treatment of the "non-radiative" piece of the metric perturbation (the piece which reduces to the monopole and dipole modes in the Schwarzschild case). This piece has a numerically important contribution to the GSF, but so far attempts to compute it via time-domain evolution have been futile due to numerical instabilities. A few ad-hoc solutions to this problem were suggested recently in Ref. [47] (including the use of a judiciously chosen generalized Lorenz-gauge in an intermediate step), but they are yet to be tested in the Kerr case.

The alternative approach is based on a *frequency domain* treatment, in which the metric perturbation is solved for mode-by-mode in a multipole-Fourier decomposition. The advantage is that one now only deals with *ordinary* differential equations,

but the method is only applicable for bound orbits of sufficiently small eccentricities. The problem of seperability in Kerr remains if one insists on working in the Lorenz gauge, but there are suggestions to overcome this using a specially designed gauge in which (1) the metric perturbation is reconstructable from curvature scalars, which obey fully separable equations in Kerr (Teukolsky's formalism); and (2) the GSF is still mathematically well-defined and physically meaningful, as it is in the Lorenz-gauge. A proposal of this kind was put forward long ago in [23], and a variant thereof is being under active development by Shah and collaborators [83, 84, 37]. This approach offers a computationally efficient route to the GSF, but much further development is needed.

Synergy with other methods:— The initial work described in Sec. 5 bears the promise of much further fruitful exchange between GSF and other computational approaches to the two-body problem, exploiting new GSF data as they become available. One of the challenges is to devise computable gauge-invariant quantities to facilitate a common language between the various approaches. Second-order GSF results, when at hand, will allow us to refine our comparisons and constrain the EOB potentials with exquisite accuracy. It is important to understand if and why the "GSFν" always provides a good (how good?) approximation even when the mass ratio is not extreme. What are the aspects of the dynamics in equal-mass binaries that can be modelled faithfully using purely perturbative methods?

GSF/PN comparison so far has been limited to circular or slightly eccentric orbits. There is merit in extending this comparison to fully eccentric orbits, which can be done using the available GSF results in Schwarzschild. Here are some specific invariant quantities that should be accessible (at least in principle) to existing Schwarzschild GSF codes, and could serve at contact points with—and strong-field benchmarks for—other approaches: (1) the GSF correction to the angular momentum and azimuthal frequency of a marginally-bound orbit on the capture threshold [64]; (2) the GSF correction to the Lyapunov exponent of unstable circular orbits below the ISCO; (3) the GSF correction to the function relating the azimuthal and radial frequencies on the "singular curve" identified in Appendix A of Ref. [60], where the transformation to orbital frequencies as system parameters becomes singular. Once GSF results in Kerr are available, one could compute the GSF correction to the Lense–Thirring precession of the orbital plane, and other spin-related effects of the GSF.

Acknowledgements

References

1. R.A. Hulse, J.H. Taylor, *Discovery of a pulsar in a binary system*, Astrophys. J. **195**, L51 (1975)
2. S.G. Hahn, R.W. Lindquist, *The Two-Body Problem in Geometrodynamics*, Ann. Phys. (N.Y.) **29**, 304 (1964)
3. L. Smarr, *Space-time generated by computers: Black holes with gravitational radiation*, Ann. N.Y. Acad. Sci. **302**, 569 (1977)
4. F. Pretorius, *Evolution of binary black-hole spacetimes*, Phys. Rev. Lett. **95**, 121101 (2005)
5. M. Campanelli, C.O. Lousto, P. Marronetti, Y. Zlochower, *Accurate evolutions of orbiting black-hole binaries without excision*, Phys. Rev. Lett. **96**, 111101 (2006)
6. J.G. Baker, J. Centrella, D.I. Choi, M. Koppitz, J. van Meter, *Gravitational-wave extraction from an inspiraling configuration of merging black holes*, Phys. Rev. Lett. **96**, 111102 (2006)
7. L. Blanchet, *Gravitational radiation from post-newtonian sources and inspiralling compact binaries*, Living Rev. Relativity **9**, lrr-2006-4 (2006). URL http://www.livingreviews.org/lrr-2006-4
8. A. Einstein, L. Infeld, B. Hoffmann, *The gravitational equations and the problem of motion*, Ann. Math. **39**, 65 (1938)
9. S. Gielen, D.K. Wise, *Spontaneously broken Lorentz symmetry for Hamiltonian gravity*, Phys. Rev. D **85**, 104013 (2012)
10. P.A.M. Dirac, *Classical theory of radiating electrons*, Proc. R. Soc. London, Ser. A **167**, 148 (1938)
11. B.S. DeWitt, *Gravitational radiation*, in *General Relativity: An Einstein Centenary Survey*, ed. by S.W. Hawking, W. Israel (Cambridge University Press, Cambridge; New York, 1979), pp. 680–745
12. R. Geroch, J. Traschen, *Strings and other distributional sources in general relativity*, Phys. Rev. D **36**, 1017 (1987)
13. LISA Project Office. URL http://lisa.nasa.gov
14. J.R. Gair, L. Barack, T. Creighton, et al., *Event rate estimates for LISA extreme mass ratio capture sources*, Class. Quantum Grav. **21**, S1595 (2004)
15. L. Barack, C. Cutler, *Using LISA extreme-mass-ratio inspiral sources to test off-Kerr deviations in the geometry of massive black holes*, Phys. Rev. D **75**, 042003 (2007)
16. Y. Mino, M. Sasaki, T. Tanaka, *Gravitational radiation reaction to a particle motion*, Phys. Rev. D **55**, 3457 (1997)
17. T.C. Quinn, R.M. Wald, *Axiomatic approach to electromagnetic and gravitational radiation reaction of particles in curved spacetime*, Phys. Rev. D **56**, 3381 (1997)
18. L. Blanchet, T. Damour, *Hereditary effects in gravitational radiation*, Phys. Rev. D **46**, 4304 (1992)
19. E. Poisson, A. Pound, I. Vega, *The motion of point particles in curved spacetime*, Living Rev. Relativity **14**(7), lrr-2011-7 (2011). URL http://www.livingreviews.org/lrr-2011-7
20. E. Gralla, R.M. Wald, *A rigorous derivation of gravitational self-force*, Class. Quantum Grav. **25**, 205009 (2008)
21. A. Pound, *Self-consistent gravitational self-force*, Phys. Rev. D **81**, 024023 (2010)
22. A.I. Harte, *Mechanics of extended masses in general relativity*, Class. Quantum Grav. **29**, 055012 (2012)
23. L. Barack, A. Ori, *Gravitational self-force and gauge transformations*, Phys. Rev. D **64**, 124003 (2001)
24. S.E. Gralla, *Gauge and averaging in gravitational self-force*, Phys. Rev. D **84**, 084050 (2011)
25. A. Pound, *Singular perturbation techniques in the gravitational self-force problem*, Phys. Rev. D **81**, 124009 (2010)
26. S. Detweiler, B.F. Whiting, *Self-force via a Green's function decomposition*, Phys. Rev. D **67**, 024025 (2003)

27. L. Barack, A. Ori, *Mode sum regularization approach for the self-force in black hole space-time*, Phys. Rev. D **61**, 061502 (2000)
28. L. Barack, *Gravitational self-force in extreme mass-ratio inspirals*, Class. Quantum Grav. **26**, 213001 (2009)
29. L. Barack, A. Ori, *Gravitational self-force on a particle orbiting a Kerr black hole*, Phys. Rev. Lett. **90**, 111101 (2003)
30. L. Barack, Y. Mino, H. Nakano, A. Ori, M. Sasaki, *Calculating the gravitational self-force in Schwarzschild spacetime*, Phys. Rev. Lett. **88**, 091101 (2002)
31. L. Barack, N. Sago, *Gravitational self-force on a particle in circular orbit around a Schwarzschild black hole*, Phys. Rev. D **75**, 064021 (2007)
32. L. Barack, N. Sago, *Gravitational self-force on a particle in eccentric orbit around a Schwarzschild black hole*, Phys. Rev. D **81**, 084021 (2010)
33. S. Akcay, *Fast frequency-domain algorithm for gravitational self-force: Circular orbits in Schwarzschild spacetime*, Phys. Rev. D **83**, 124026 (2011)
34. N. Warburton, S. Akcay, L. Barack, J.R. Gair, N. Sago, *Evolution of inspiral orbits around a Schwarzschild black hole*, Phys. Rev. D **85**, 061501 (2012)
35. N. Warburton, L. Barack, *Self-force on a scalar charge in Kerr spacetime: Circular equatorial orbits*, Phys. Rev. D **81**, 084039 (2010)
36. N. Warburton, L. Barack, *Self-force on a scalar charge in Kerr spacetime: Eccentric equatorial orbits*, Phys. Rev. D **83**, 124038 (2011)
37. A.G. Shah, J.L. Friedman, T.S. Keidl, *Extreme-mass-ratio inspiral corrections to the angular velocity and redshift factor of a mass in circular orbit about a Kerr black hole*, Phys. Rev. D **86**, 084059 (2012)
38. A. Heffernan, A. Ottewill, B. Wardell, *High-order expansions of the Detweiler-Whiting singular field in Schwarzschild spacetime*, Phys. Rev. D **86**, 104023 (2012)
39. A. Heffernan, A. Ottewill, B. Wardell, *High-order expansions of the Detweiler-Whiting singular field in Kerr spacetime*, ArXiv e-prints [arXiv:1211.6446 [gr-qc]] (2012)
40. L. Barack, D.A. Golbourn, *Scalar-field perturbations from a particle orbiting a black hole using numerical evolution in $2+1$ dimensions*, Phys. Rev. D **76**, 044020 (2007)
41. L. Barack, D.A. Golbourn, N. Sago, *m-mode regularization scheme for the self-force in Kerr spacetime*, Phys. Rev. D **76**, 124036 (2007)
42. I. Vega, S. Detweiler, *Regularization of fields for self-force problems in curved spacetime: Foundations and a time-domain application*, Phys. Rev. D **77**, 084008 (2008)
43. S.R. Dolan, L. Barack, B. Wardell, *Self-force via m-mode regularization and 2+1D evolution. II. Scalar-field implementation on Kerr spacetime*, Phys. Rev. D **84**, 084001 (2011)
44. B. Wardell, I. Vega, J. Thornburg, P. Diener, *Generic effective source for scalar self-force calculations*, Phys. Rev. D **85**, 104044 (2012)
45. I. Vega, P. Diener, W. Tichy, S. Detweiler, *Self-force with $(3+1)$ codes: A primer for numerical relativists*, Phys. Rev. D **80**, 084021 (2009)
46. S.R. Dolan, L. Barack, *Self-force via m-mode regularization and $2+1$D evolution: Foundations and a scalar-field implementation on Schwarzschild spacetime*, Phys. Rev. D **83**, 024019 (2011)
47. S.R. Dolan, L. Barack, *Self-force via m-mode regularization and 2+1D evolution: III. Gravitational field on Schwarzschild spacetime*, ArXiv e-prints [arXiv:1211.4586 [gr-qc]] (2012)
48. S. Dolan, L. Barack, *Self-force via m-mode regularization and 2+1D evolution: IV. Gravitational field on Kerr spacetime*. In preparation
49. P. Diener, I. Vega, B. Wardell, S. Detweiler, *Self-consistent orbital evolution of a particle around a Schwarzschild black hole*, Phys. Rev. Lett. **108**, 191102 (2012)
50. P. Cañizares, C.F. Sopuerta, *Efficient pseudospectral method for the computation of the self-force on a charged particle: Circular geodesics around a Schwarzschild black hole*, Phys. Rev. D **79**, 084020 (2009)
51. J. Thornburg, *Adaptive mesh refinement for characteristic grids*, Gen. Rel. Grav. **43**, 1211 (2011)
52. A. Zenginoglu, *Hyperboloidal layers for hyperbolic equations on unbounded domains*, J. Comput. Phys. **230**, 2286 (2011)

53. C. Darwin, *The gravity field of a particle*, Proc. R. Soc. London, Ser. A **249**, 180 (1959)
54. A. Pound, E. Poisson, *Multiscale analysis of the electromagnetic self-force in a weak gravitational field*, Phys. Rev. D **77**, 044012 (2008)
55. J.R. Gair, É. Flanagan, S. Drasco, T. Hinderer, S. Babak, *Forced motion near black holes*, Phys. Rev. D **83**, 044037 (2011)
56. S.L. Detweiler, *Perspective on gravitational self-force analyses*, Class. Quantum Grav. **22**, S681 (2005)
57. S. Detweiler, *Consequence of the gravitational self-force for circular orbits of the Schwarzschild geometry*, Phys. Rev. D **77**, 124026 (2008)
58. L. Blanchet, S. Detweiler, A. Le Tiec, B.F. Whiting, *Post-Newtonian and numerical calculations of the gravitational self-force for circular orbits in the Schwarzschild geometry*, Phys. Rev. D **81**, 064004 (2010). Erratum: ibid. **81**, 084033 (2010)
59. N. Sago, L. Barack, S. Detweiler, *Two approaches for the gravitational self-force in black hole spacetime: Comparison of numerical results*, Phys. Rev. D **78**, 124024 (2008)
60. L. Barack, N. Sago, *Beyond the geodesic approximation: Conservative effects of the gravitational self-force in eccentric orbits around a Schwarzschild black hole*, Phys. Rev. D **83**, 084023 (2011)
61. L. Barack, A. Le Tiec, N. Sago, In progress
62. L. Barack, N. Sago, *Gravitational self-force correction to the innermost stable circular orbit of a Schwarzschild black hole*, Phys. Rev. Lett. **102**, 191101 (2009)
63. S. Akcay, L. Barack, T. Damour, N. Sago, *Gravitational self-force and the effective-one-body formalism between the innermost stable circular orbit and the light ring*, Phys. Rev. D **86**, 104041 (2012)
64. T. Damour, *Gravitational self-force in a Schwarzschild background and the effective one-body formalism*, Phys. Rev. D **81**, 024017 (2010)
65. L. Barack, C.O. Lousto, *Perturbations of Schwarzschild black holes in the Lorenz gauge: Formulation and numerical implementation*, Phys. Rev. D **72**, 104026 (2005)
66. M. Favata, *Conservative self-force correction to the innermost stable circular orbit: Comparison with multiple post-Newtonian-based methods*, Phys. Rev. D **83**, 024027 (2011)
67. C.O. Lousto, H. Nakano, Y. Zlochower, M. Campanelli, *Statistical studies of spinning black-hole binaries*, Phys. Rev. D **81**, 084023 (2010)
68. A. Buonanno, T. Damour, *Effective one-body approach to general relativistic two-body dynamics*, Phys. Rev. D **59**, 084006 (1999)
69. L. Barack, T. Damour, N. Sago, *Precession effect of the gravitational self-force in a Schwarzschild spacetime and the effective one-body formalism*, Phys. Rev. D **82**, 084036 (2010)
70. A. Le Tiec, A.H. Mroué, L. Barack, et al., *Periastron advance in black-hole binaries*, Phys. Rev. Lett. **107**, 141101 (2011)
71. A. Le Tiec, L. Blanchet, B.F. Whiting, *First law of binary black hole mechanics in general relativity and post-Newtonian theory*, Phys. Rev. D **85**, 064039 (2012)
72. E. Barausse, A. Buonanno, A. Le Tiec, *Complete nonspinning effective-one-body metric at linear order in the mass ratio*, Phys. Rev. D **85**, 064010 (2012)
73. E. Barausse, V. Cardoso, G. Khanna, *Testing the cosmic censorship conjecture with point particles: The effect of radiation reaction and the self-force*, Phys. Rev. D **84**, 104006 (2011)
74. C. Gundlach, S. Akcay, L. Barack, A. Nagar, *Critical phenomena at the threshold of immediate merger in binary black hole systems: The extreme mass ratio case*, Phys. Rev. D **86**, 084022 (2012)
75. A. Pound, *Second-order gravitational self-force*, Phys. Rev. Lett. **109**, 051101 (2012)
76. A. Pound, *Nonlinear gravitational self-force: Field outside a small body*, Phys. Rev. D **86**, 084019 (2012)
77. S.E. Gralla, *Second-order gravitational self-force*, Phys. Rev. D **85**, 124011 (2012)
78. T. Hinderer, É. Flanagan, *Two-timescale analysis of extreme mass ratio inspirals in Kerr spacetime: Orbital motion*, Phys. Rev. D **78**, 064028 (2008)
79. A. Pound, *Singular perturbation techniques in the gravitational self-force problem*, Phys. Rev. D **81**, 124009 (2010)

80. J. Gair, N. Yunes, C.M. Bender, *Resonances in extreme mass-ratio inspirals: Asymptotic and hyperasymptotic analysis*, J. Math. Phys. **53**, 032503 (2012)
81. É. Flanagan, T. Hinderer, *Transient resonances in the inspirals of point particles into black holes*, Phys. Rev. Lett. **109**, 071102 (2012)
82. É. Flanagan, S.A. Hughes, U. Ruangsri, *Resonantly enhanced and diminished strong-field gravitational-wave fluxes*, ArXiv e-prints [arXiv:1208.3906 [gr-qc]] (2012)
83. T.S. Keidl, A.G. Shah, J.L. Friedman, D.H. Kim, L.R. Price, *Gravitational self-force in a radiation gauge*, Phys. Rev. D **82**, 124012 (2010)
84. A.G. Shah, T.S. Keidl, J.L. Friedman, D.H. Kim, L.R. Price, *Conservative, gravitational self-force for a particle in circular orbit around a Schwarzschild black hole in a radiation gauge*, Phys. Rev. D **83**, 064018 (2011)